Eur. Phys. J. D (2015) 69: 174
DOI: 10.1140/epjd/e2015-60157-9

THE EUROPEAN PHYSICAL JOURNAL D

Regular Article

Internuclear interaction and distortion effects on fully differential cross section for single ionization of helium by 100 MeV/amu C^{6+} impact

Wenfang An, Chenwen Lu, Shiyan Sun, and Xiangfu Jia[a]

School of Physics and Information Engineering, Shanxi Normal University, Linfen, Shanxi 041004, P.R. China

Received 7 March 2015 / Received in final form 8 June 2015
Published online 14 July 2015 –

Abstract. The modified Coulomb-Born approximation model is applied to calculate the fully differential cross section (FDCS) for single ionization of helium by 100 MeV/amu C^{6+} impact. We study the influence of the internuclear interaction on the FDCS in the scattering plane and the perpendicular plane. Comparisons are made with absolute experimental data and the 3DW results and we find that our calculations with (without) the internuclear interaction yield excellent agreement with experiments for the small (large) momentum transfer. Accordingly, we discuss the contributions of distortion effects to the FDCS both in the scattering plane and the perpendicular plane. It turns out that the distortion effects become significantly important with increasing momentum transfer.

1 Introduction

As the continuous development of the experimental technique known as COLTRIMS (cold-target recoil-ion momentum spectroscopy) [1], the fully differential cross section (FDCS) for heavy-ion impact ionization can now be measured in different geometries [2,3], thus posing a great challenge to the theory. Particularly for 100 MeV/amu C^{6+} single ionization of helium, unexpected results were found both in and out of the scattering plane (defined by the initial and final projectile momenta). In the scattering plane for small and intermediate momentum transfer, the experimental data was in good agreement with theory, as would be expected for a high-energy collision. However, some considerable discrepancies were found for large momentum transfer. Furthermore, the experimental structure out of the scattering plane was not well reproduced by most of the existing theoretical models, ranging from the first Born approximation (FBA) [4], three-body distorted-wave (3DW) [5,6] to coupled-pseudostate (CP) [7] and fully quantum-mechanical convergent close-coupling (CCC) models [8]. Although many physical effects including high-order effects [9,10] or, most recently, interference effects [11,12], has been taken into account in some models, to remove this discrepancy, all the possible explanations cannot give a satisfactory result. Consequently, the new physical effects are necessary to shed more light on the problem. In addition, a factor which may affect the results of the theoretical calculations is the distorting potential. However, to our best knowledge, none of these calculations has examined this issue in detail.

[a] e-mail: jiaxf@dns.sxnu.edu.cn

In this paper,we use a perturbation method called the modified Coulomb-Born (MCBPT) approximation, which has been previously introduced in detail in reference [13], to analyze the problem mentioned above. It is worthy noting that this model is based on a four-body theory and, most importantly, the distorting potential is taken into account in the initial channel, as a result, a proper connection between the entrance channel asymptotic state and the corresponding perturbation potential is established in our calculation (details are contained in the next section). Our purpose is to assess the ability of the present model to reproduce the experimental data and explore the role of the internuclear interaction (PT) in the single ionization process. It turns out that our calculation without the internuclear interaction (MCB) is in very good agreement with experiment for large momentum transfer, whereas other theoretical models do not. Moreover, we analyze the physical origin of the features in the FDCS and find that the signatures of the distortion effects are revealed. In particular, the importance of the distortion effects in determining the magnitude of the FDCS is demonstrated. Atomic units are used throughout unless otherwise stated.

2 Theoretical treatments

Let us consider a bare ion of nuclear charge Z_p impacting a helium atom in the ground state and ionizing an electron. In the center-of-mass (CM) system, the FDCS may be written as:

$$\frac{d^3\sigma}{d\Omega_p d\Omega_e dE_e} = N_e(2\pi)^4\mu^2 p\frac{k_f}{k_i}|T_{fi}^{-}|^2, \qquad (1)$$

where N_e is the number of electrons in the atomic shell. The solid angles $d\Omega_p$ and $d\Omega_e$ represent the direction of scattering of the projectile and the ejected electron, respectively. The initial and final momenta of the projectile are k_i and k_f, the ejected-electron's energy and momentum are given by E_e and p respectively. μ is the reduced mass of the projectile-target atom system.

The prior form of the exact transition matrix (T-matrix) in the distorted wave formalism is given by:

$$T_{fi}^{-} = \langle \Psi_f^{-} | V_i' | \chi_i^{+} \rangle, \tag{2}$$

here,

$$V_i' = V_i - V_{id}, \tag{3}$$

V_{id} ought to be connected with χ_i^+, but otherwise is temporarily considered as being an arbitrary distorting potential operator, Ψ_f^- is the approximate final-state four-body wavefunction. Hence, equation (2) can be rewritten as:

$$T_{fi}^{-} = T_{vi} + T_{vd}, \tag{4}$$

here T_{vi} and T_{vd} stem respectively from the perturbation potential V_i and the distorting potential V_{id}.

In the initial channel, one may write:

$$H_i = -\frac{1}{2\mu}\nabla_r^2 - \frac{1}{2b}\nabla_{x_1}^2 - \frac{1}{2b}\nabla_{x_2}^2 - \frac{Z_T}{x_1} - \frac{Z_T}{x_2} + \frac{1}{x_{12}}, \tag{5}$$

$$V_i = -\frac{Z_p}{s_1} - \frac{Z_p}{s_2} + \frac{Z_P Z_T}{R}, \tag{6}$$

where H_i represents the Hamiltonian in the entrance channel, and V_i is the corresponding perturbation potential. $\mathbf{r}$ is the position vector of the projectile relative to the atomic center of mass. $\mathbf{x}_1$ and $\mathbf{x}_2$ represent the position vectors of the active and passive electrons with respect to the target core. $\mathbf{s}_1$ and $\mathbf{s}_2$ represent the position vectors of the active and passive electrons with respect to the projectile. $\mathbf{R}$ and $\mathbf{x}_{12}$ are the vectors of the internuclear and interelectronic axis. The charges of the target nucleus are given by Z_T. b is the reduced mass of each electron relative to the atomic core ($b \approx 1$). The initial state distorted wave χ_i^+ is defined by:

$$(H_i + V_{id} - E)\chi_i^{+} = 0, \tag{7}$$

here, E is the total energy of the whole system. Much better approximations can be made for χ_i^+ such as eikonal-initial-state approximation (EIS) introduced by Belkic [13]

$$\chi_i^{+} = \phi_i \exp[-i\alpha_0 \ln(vs_1 + \mathbf{v}\cdot\mathbf{s}_1) + i\alpha_0' \ln(vR - \mathbf{v}\cdot\mathbf{R})], \tag{8}$$

where $\alpha_0 = \frac{Z_p}{v}$, $\alpha_0' = \frac{Z_p Z_T'}{v}$ and $Z_T' = Z_T - 1$. The initial wave vector labeled by $\mathbf{k}_i$ is defined via $\mathbf{k}_i = \mu\mathbf{v}$, where $\mathbf{v}$ is the velocity of the incident projectile with respect to the target. This state thus includes the projectile-electron and projectile-target ion interactions approximately in the initial channel. The unperturbed state ϕ_i in the entrance channel is given by:

$$\phi_i = (2\pi)^{-3/2} \exp(i\mathbf{k}_i \cdot \mathbf{r})\phi(x_1, x_2). \tag{9}$$

For the bound-state wavefunction $\phi(x_1, x_2)$, in reference [14], Ghanbari-Adivi et al. applied three different wave functions to describe the helium atoms in their ground states and investigate the influence of the static electron correlations on the ionization process. It turns out that, to some extent, the static electronic correlation has a significant influence on the ionization process and the correlated four-parameter Byron and Joachain wave function in provided better results in the binary-peak region. Thus, we have chosen the analytical fit to the Hartree-Fock wave function given by Byron and Joachain [15],

$$\phi(x_1, x_2) = U(x_1)U(x_2), \tag{10}$$

where $U(x) = (4\pi)^{-1/2}(2.60505e^{-1.41x} + 2.08144e^{-2.61x})$.

With the help of the total Hamiltonian of this system, i.e. $H = H_i + V_i$, we can rewrite equation (7) in the equivalent form:

$$(H - E)\left|\chi_i^{+}\right\rangle = V_i'\left|\chi_i^{+}\right\rangle, \tag{11}$$

inserting (8) into equation (11) and resorting to the usual mass limit $\mu \gg 1$, one readily identifies the additional distorting potential V_{id} as:

$$V_{id} = \frac{\alpha_0' v}{R} - \frac{\alpha_0 v}{s_1} - \frac{\alpha_0 Z_p}{s_1}\frac{1}{vs_1 + \mathbf{v}\cdot\mathbf{s}_1} - \frac{i\alpha_0}{s_1}\frac{1}{vs_1 + \mathbf{v}\cdot\mathbf{s}_1}\nabla_{x_1}(\ln\phi)\cdot[v\mathbf{s}_1 + s_1\mathbf{v}]. \tag{12}$$

The final state wavefunction Ψ_f^- is given by a product of the ground-state wave function of helium ion and the approximate three-Coulomb wave

$$\Psi_f^{-}(\mathbf{x}_1, \mathbf{x}_2, \mathbf{R}) = \phi_f(\mathbf{x}_2)\Psi^{-}(\mathbf{x}_1, \mathbf{R}), \tag{13}$$

where Ψ^- can be expressed as [16,17]:

$$\Psi^{-}(\mathbf{x}_1, \mathbf{R}) \approx (2\pi)^{-3}\exp[i(\mathbf{k}_f\cdot\mathbf{R} + \mathbf{p}\cdot\mathbf{x}_1)] \times \chi_f(\alpha_{PT}, \mathbf{k}_f, \mathbf{R})\chi_e(\alpha_{Te}, \mathbf{p}, \mathbf{x}_1) \times \chi(\alpha_{Pe}, \mathbf{K}, \mathbf{s}_1). \tag{14}$$

here $\mathbf{K}$ and $\mathbf{p}$ is the momentum of the ejected-electron with respect to the projectile and target core, respectively. χ_f and χ_e are the distorted waves for the scattered projectile and ejected electron respectively. The Coulomb distorted factor is given by:

$$\chi(\alpha, k, r) = e^{(-\pi\alpha/2)}\Gamma(1 - i\alpha)\,{}_1F_1(i\alpha; 1; -i(kr + \mathbf{k}\cdot\mathbf{r})), \tag{15}$$

the symbols Γ and ${}_1F_1$ represent the gamma function and the confluent hypergeometric function, respectively. The Sommerfeld parameters have the form

$$\alpha_{PT} = \frac{\mu Z_P Z_\infty}{k_f},\ \alpha_{Pe} = -\frac{Z_P}{K},\ \alpha_{Te} = -\frac{Z_\infty}{p}. \tag{16}$$

The resulting prior form of the transition amplitude is then obtained from equation (2) as:

$$T_{fi}^{-} = N \int\int\int d\mathbf{r} d\mathbf{x}_1 d\mathbf{x}_2 \phi_{nl}(x_2) e^{i\mathbf{q}\cdot\mathbf{r} - i\mathbf{p}\cdot\mathbf{x}_1} \times \chi_f^*(\alpha_{PT}, \mathbf{k}_f, \mathbf{R}) \chi_e^*(\alpha_{Te}, \mathbf{p}, \mathbf{x}_1) \chi^*(\alpha_{Pe}, \mathbf{K}, \mathbf{s}_1) \times \left\{ V_i - \frac{\alpha_0' v}{R} + \frac{\alpha_0 v}{s_1} + \frac{\alpha_0 Z_p}{s_1} \frac{1}{v s_1 + \mathbf{v}\cdot\mathbf{s}_1} + \frac{i\alpha_0}{s_1} \frac{1}{v s_1 + \mathbf{v}\cdot\mathbf{s}_1} \nabla_{x_1}(\ln\phi) \cdot [v\mathbf{s}_1 + s_1 \mathbf{v}] \right\} \times \frac{(vR - \mathbf{v}\cdot\mathbf{R})^{i\alpha_0'}}{(v s_1 + \mathbf{v}\cdot\mathbf{s}_1)^{i\alpha_0}} \phi^-(x_1, x_2), \quad (17)$$

with $\mathbf{q} = \mathbf{k}_i - \mathbf{k}_f$ (momentum transfer), and

$$N = (2\pi)^{-3} (2\pi)^{-\frac{3}{2}} e^{(-\pi\alpha_{Pe}/2)} e^{(-\pi\alpha_{Te}/2)} e^{(-\pi\alpha_{PT}/2)} \times \Gamma(1 + i\alpha_{Pe}) \Gamma(1 + i\alpha_{Te}) \Gamma(1 + i\alpha_{PT}). \quad (18)$$

In the asymptotic scattering region, the vectorial relation

$$\mathbf{r} = \frac{M_T + 1}{M_T + 2}\mathbf{x}_1 - \frac{1}{M_T + 2}\mathbf{x}_2 - \mathbf{s}_1$$

simplifiesas $\mathbf{r} \mid_{r\to\infty} \approx \mathbf{R} = \mathbf{x}_1 - \mathbf{s}_1$, which is further reduced to $\mathbf{r} \mid_{r\to\infty} \approx -\mathbf{s}_1$, since x_1 is of the order of Bohr radius and s_1 is large. The x_1-, x_2-, and r-integrals (17) can be calculated analytically with the standard methods by employing the real integral representation for the Coulomb phases in reference [18] and the confluent hypergeometric function in reference [19]. The nine-dimensional integral (17) can be reduced analytically, and without any further approximation, to a four-dimensional integral on the real parameters which has to be carried out numerically. The convergence of each integral has been tested properly and the final results are supposed to be accurate up to data provided in the figures quoted in Section 3.

In this model, the most important component is that a proper connection between the entrance channel asymptotic state and the corresponding perturbation potential is established by an additional distorting potential (see Eq. (12)). Also, all three two-body interactions are treated on equal footing in equation (14). An uncertain point of this model represents the use of the asymptotic charge $Z_\infty = 1$. We label the present calculation using the above wavefunctions, potentials and T-matrix (2) as MCBPT theory to distinguish the previous MCB calculations (details are contained in the Appendix of Ref. [13]). The important distinctions are:

(1) The previous MCB calculations performed by Belkic (1997) used a straight-line semi-classical trajectory for the projectile while we use a full quantum-mechanical treatment. A good result for the total cross section was found, with the semiclassical way in the previous MCB calculations [13]. In this work, the FDCS are calculated for the first time with a quantum-mechanical MCBPT approach.

(2) Our MCBPT theory contains the internuclear interaction (the PT interaction) in both the initial and final channels (see Eqs. (8) and (14)), whereas the previous MCB calculations don not.

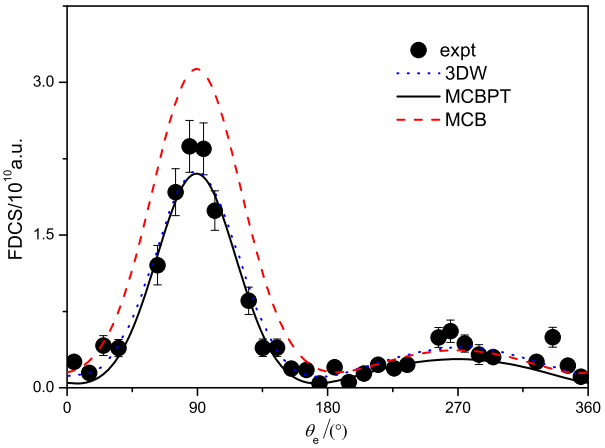

Fig. 1. The FDCS for single ionization of helium by 100 MeV/amu C^{6+} in the scattering plane. The electron emission energy $E_e = 6.5$ eV and the momentum transfer $q = 0.88$ a.u. The angle θ_e is the emission angle of the electron. Solid line: MCBPT. Dashed line: MCB. Dotted line: 3DW [5]. Solid circles: experimental data [4].

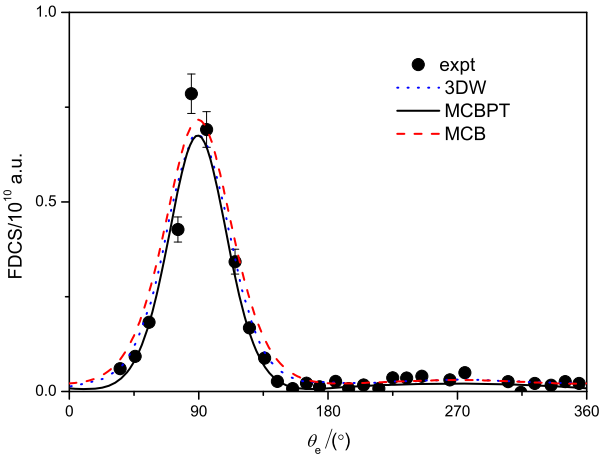

Fig. 2. Same as Figure 1 expect that the momentum transfer is 1.43 a.u. and the ejected electron energy is 17.5 eV.

To explore the impact of the PT interaction on the FDCS, we have evaluated the FDCS with the PT interaction turned off ($\alpha_0' = 0, \alpha_{PT} = 0$, see Eqs. (8) and (14)) to show how important is to adequately model this interaction in a single ionization process.

3 Results and discussion

To check the accuracy of the MCBPT method, the FDCS are calculated, using equation (1), for 100 MeV/amu C^{6+} impact ionization of helium both in the scattering plane and the perpendicular plane. Comparisons are made with the corresponding experimental measurements [4] and the 3DW of Madison et al. [5]. The role of the PT interaction is analyzed. The results are displayed in Figures 1–5. And

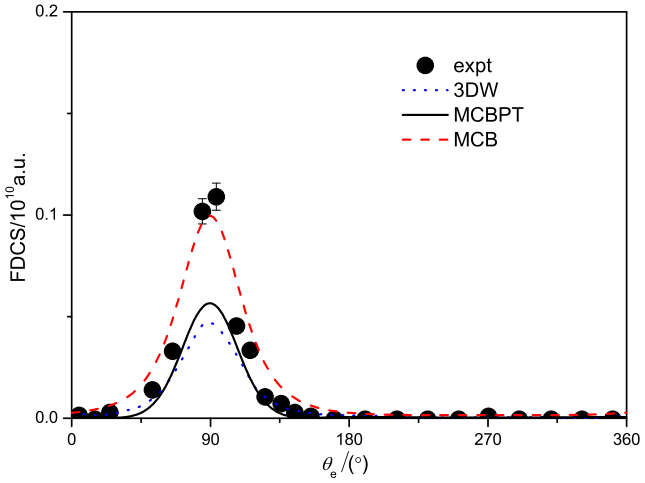

Fig. 3. Same as Figure 1 except that the momentum transfer is 2.65 a.u. and the ejected electron energy is 37.5 eV.

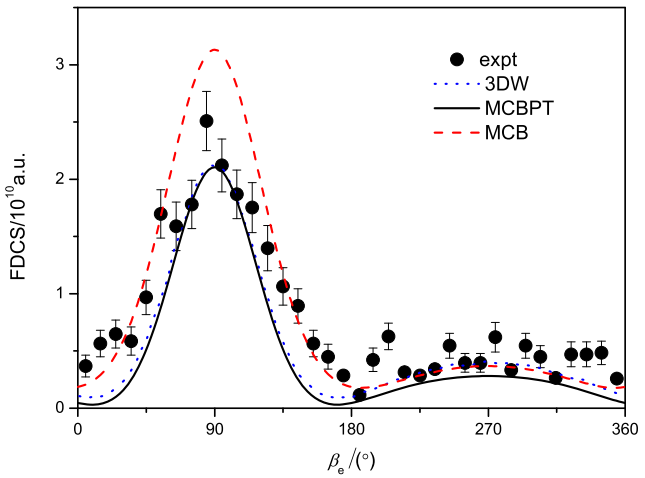

Fig. 4. Same as Figure 1 but the cross section is given in the plane perpendicular to the incident beam direction, containing the momentum transfer q. The angular dependence for the perpendicular plane is β_e defined as $\beta_e = \frac{\pi}{2} - \varphi_e$, φ_e is the azimuthal angle for the ionized electron.

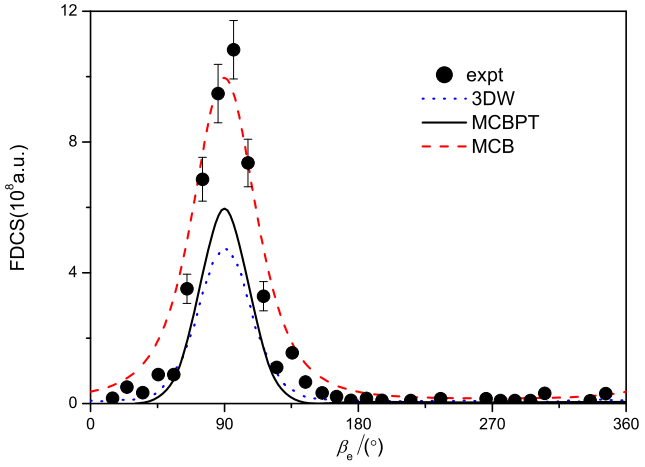

Fig. 5. Same as Figure 4 except that the momentum transfer is 2.65 a.u. and the ejected electron energy is 37.5 eV.

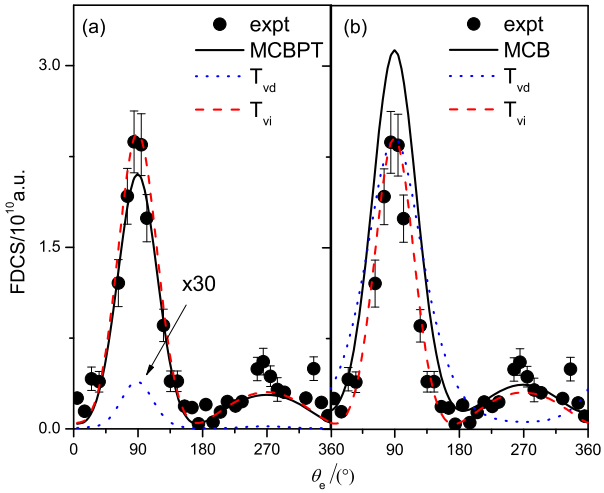

Fig. 6. The same geometry as in Figure 1. The solid lines represent the MCBPT result (left column) and MCB result (right column). The incoherent contributions to the FDCS of the perturbation potential scattering amplitude T_{vi} (dash lines) and distortion potential scattering amplitude T_{vd} (dotted lines), and the coherent sum of T_{vi} and T_{vd} (solid lines).

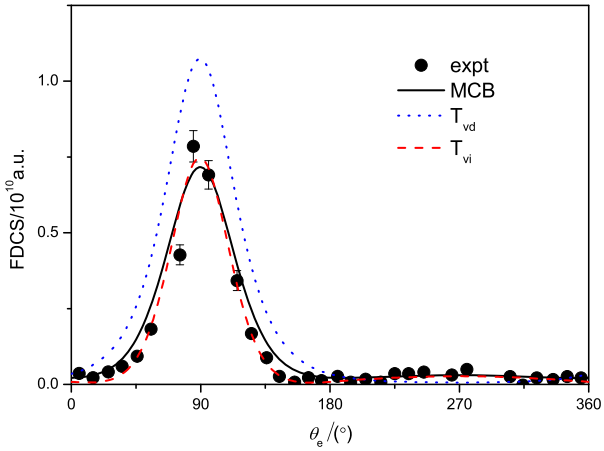

Fig. 7. Same as Figure 6 except that the momentum transfer is 1.43 a.u. and the ejected electron energy is 17.5 eV.

the contributions of distortion effects to the FDCS are investigated in Figures 6–10.

In Figures 1–5 we observe familiar structures: at the lower momentum transfer (Figs. 1 and 4) the emission pattern clearly exhibits the so-called binary and recoil peaks; at higher momentum transfer (Figs. 3 and 5) the recoil peak rapidly disappears. Although all theories show the main features of the experimental data, the discrepancy in the absolute magnitude occurs between the theoretical methods.

In the scattering plane, for small and intermediate momentum transfer (Figs. 1 and 2) the MCBPT calculations are in good agreement with the experiment, as the same as the 3DW results. However, for large momentum transfer (see Fig. 3), significant discrepancies were found in the MCBPT and 3DW approximations, with the MCBPT being somewhat better. Amazingly, when the PT interaction

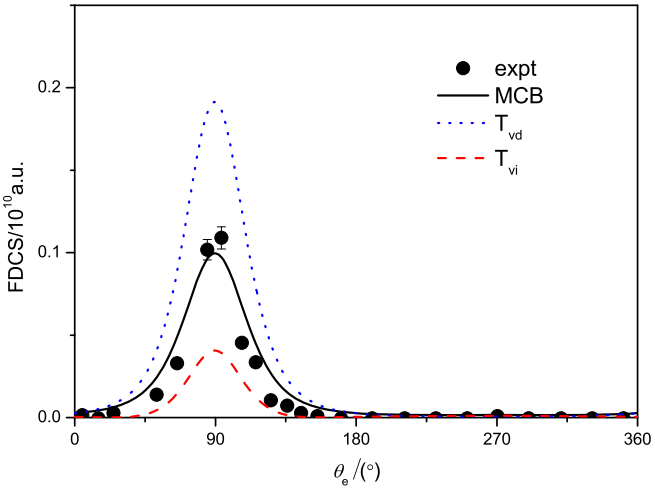

Fig. 8. Same as Figure 6 except that the momentum transfer is 2.65 a.u. and the ejected electron energy is 37.5 eV.

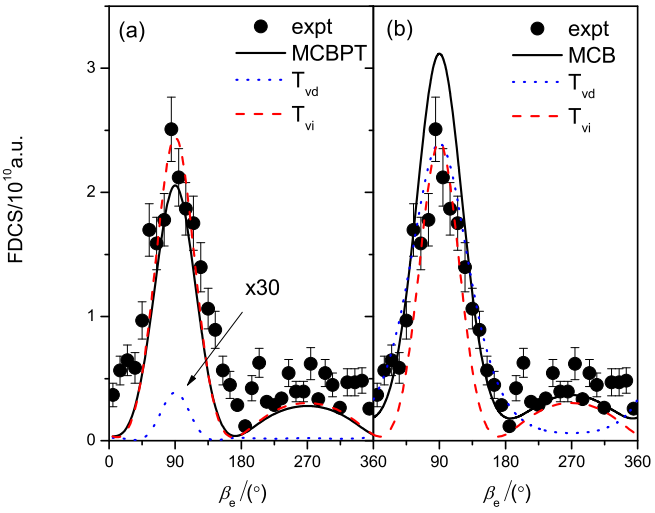

Fig. 9. Same as Figure 6 but the cross section is given in the perpendicular plane.

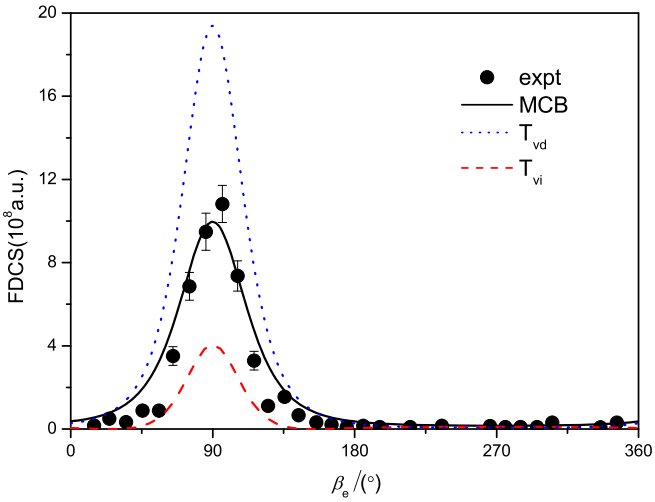

Fig. 10. Same as Figure 9 except that the momentum transfer is 2.65 a.u. and the ejected electron energy is 37.5 eV.

is turned off (MCB), the discrepancy vanishes and a nearly perfect agreement with the experiment is obtained both in magnitude and shape. Furthermore, the same behaviour is also observed in the perpendicular plane (Figs. 4 and 5). It indicates that, on the one hand, the present theory (MCBPT) based on a four-body model gives a significant improvement over a three-body model (3DW), especially for large momentum transfer, large improvement is achieved with the MCB model compared to the 3DW calculations. On the other hand, at small momentum transfer the PT interaction seems to be more important in the calculation that gives better results, while at large momentum transfer the neglect of the PT interaction indeed leads to an excellent agreement with the experiment. Furthermore, at small momentum transfer, this observation seems to be contrary to previous studies [8,20] and even in conflict with a simple model which describes the PT interaction in terms of classical Rutherford scattering at large momentum transfer.

To explore the physical origin of the peak structure for the FDCS in the scattering plane and the perpendicular plane, we examine the contributions of the scattering amplitudes from perturbation and distorting potentials to the FDCS using MCB and MCBPT models. From Figure 6, we observe that the incoherent contribution of the T_{vi} to the cross section is equal in the two calculations. It is worthy noting that the contribution to the cross section of the scattering amplitude T_{vd} is very small so it has been multiplied by a factor of 30 in the MCBPT model (Fig. 6a), but this contribution rapidly increases when the PT interaction is turned off (Fig. 6b). And the constructive interference of the two scattering amplitudes (see Eq. (4)) overestimate the binary peak of the experiment in the MCB model, in other words, the distortion effect is strengthened as a consequence of lacking an account for the PT interaction. It indicates that it is likely that the PT interaction have a tendency of weakening the distortion effects (see Eq. (12)). This can be understood as follows: at small momentum transfer favours large impact parameter collisions, leading to a weaker distortion effect than what is taken into account in the MCB model, and while only the PT interaction is incorporated, the distortion effect is reduced and it is well described by the MCBPT calculation (Fig. 6a). Moreover, the same theoretical analysis also applies to the intermediate momentum transfer (Fig. 7). It indicates that indeed the effect due to the PT interaction has a tendency of counteracting the distortion effect. Therefore, in our MCBPT calculation the PT interaction is necessary in order to weaken distortion effects at small momentum transfer. However, with increasing momentum transfer (the impact parameter becomes smaller and smaller), the distortion effect increases quickly and it is exactly described by the cross section arising from the destructive interference between T_{vi} and T_{vd} (see Fig. 8). As a result, the PT interaction must be neglected, otherwise the distortion effect would be largely weakened by the effect due to the PT interaction, as found in MCBPT calculation of Figure 3. It is demonstrated that with increasing momentum transfer the distortion effects become

more and more important. In addition, for recoil peak, the peak structure are primarily determined by the amplitude T_{vi} and then modified by the amplitude T_{vd}.

In order to further elucidate the conclusion presented above, we now consider electron emission in the plane perpendicular to the scattering plane. Like for the scattering plane, the signatures of the distortion effect are also revealed in the perpendicular plane. As mentioned above, for small momentum transfer the distortion effect is not obvious, thus a good result is obtained in the MCBPT theory (Fig. 9a). In contrast, in the MCB model the distortion effect is not counteracted by the PT interaction so that the binary peak of the experiment is overestimated by the constructive interference between T_{vi} and T_{vd} (Fig. 9b). It also indicates that the potential interference effect is unimportant in this case, which is in accord with the results of references [21,22]. For the case of large momentum transfer (see Fig. 10) the dominant incoherent contribution to the cross section comes from the scattering amplitude T_{vd} and the destructive interference between T_{vi} and T_{vd} yields an excellent agreement with experiments, because the distortion effect is not weakened by the higher-order interaction PT. Therefore, a similar conclusion within the scattering plane is that with increasing momentum transfer the distortion effects become significantly important and indeed both effects caused by the PT interaction and the distorting potential can cancel each other.

4 Conclusion

We have carried out calculations of the FDCS for single ionization of helium by 100 MeV/amu C^{6+} projectiles using MCBPT approximation in both the scattering plane and the perpendicular plane. The role of the PT interaction is analyzed by comparing the results of the MCB and MCBPT. It is found that the MCBPT theory yields better results for small momentum transfer and the MCB calculations are in very good agreement with experiments for large momentum transfer. It is demonstrated that with increasing momentum transfer the PT interaction become significantly less important.

We have also presented the physical origin of the features in the FDCS using the present MCB and MCBPT models in the scattering and perpendicular planes. It is shown that for small momentum transfer, the good result observed in the MCBPT calculation is due to a cancellation of the distortion effects by the higher-order effects PT. Thus the distortion effects are overestimated by the MCB model. For large momentum transfer the experimental data is excellently reproduced by the destructive interference of T_{vi} and T_{vd} both in the scattering plane and perpendicular plane, because the distortion effects are not weakened by the higher-order effects PT. It indicates that the distortion effects are not pronounced at small momentum transfer, but it is crucially important at the large momentum transfer. Consequently, our MCB model is more probably suitable for large momentum transfer and high electron emission energy due to accounting for distortion effects. Most importantly, an appropriate combination of the higher-order effects PT and distortion effects is worth paying much attention to. Furthermore, it also provides a valuable indication that the selection of the distorting potential may be an important component for the future theoretical treatment of the atomic few-body problem. This will be the direction of our future work.

Project supported by the National Natural Science Foundation of China (Grant No. 11274215), the Natural Science Foundation of Shanxi Province, China (Grant No. 2010011009).

References

1. R. Moshammer, J. Ullrich, M. Unverzagt, W. Schmidt, P. Jardin, R.E. Olson, R. Mann, R. Dörner, V. Mergel, U. Buck, H. Schmidt-Böcking, Phys. Rev. Lett. **73**, 3371 (1994)
2. M. Schulz, R. Moshammer, D.H. Madison, R.E. Olson, P. Marchalant, C.T. Whelan, H.R.J. Walters, S. Jones, M. Foster, H. Kollmus, A. Cassimi, J. Ullrich, J. Phys. B **34**, L305 (2001)
3. D. Fischer, R. Moshammer, M. Schulz, A. Voitkiv, J. Ullrich, J. Phys. B **36**, 3555 (2003)
4. M. Schulz, R. Moshammer, D. Fischer, H. Kollmus, D.H. Madison, S. Jones, J. Ullrich, Nature **422**, 48 (2003)
5. D. Madison, M. Schulz, S. Jones, M. Foster, R. Moshammer, J. Ullrich, J. Phys. B **35**, 3297 (2002)
6. A.L. Harris, D.H. Madison, J.L. Peacher, M. Foster, K. Bartschat, H.P. Saha, Phys. Rev. A **75**, 032718 (2007)
7. H.R.J. Walters, C.T. Whelan, Phys. Rev. A **85**, 062701 (2012)
8. I.B. Abdurakhmanov, I. Bray, D.V. Fursa, A.S. Kadyrov, A.T. Stelbovics, Phys. Rev. A **86**, 034701 (2012)
9. J. Colgan, M.S. Pindzola, F. Robicheaux, M.F. Ciappina, J. Phys. B **44**, 175205 (2011)
10. M.F. Ciappina, W.R. Cravero, M. Schulz, J. Phys. B **45**, 2577 (2007)
11. K.N. Egodapitiya, S. Sharma, A. Hasan, A.C. Laforge, D.H. Madison, R. Moshammer, M. Schulz, Phys. Rev. Lett. **106**, 153202 (2011)
12. X.Y. Ma, X. Li, S.Y. Sun, X.F. Jia, Europhys. Lett. **98**, 53001 (2012)
13. Dz. Belkic, Nucl. Instrum. Methods Phys. Res. B **124**, 365 (1997)
14. E. Ghanbari-Adivi, S. Eskandari, Chin. Phys. B **1**, 013401 (2015)
15. F.W. Byron Jr, C.J. Joachain, Phys. Rev. **146**, 1 (1966)
16. C.R. Garibotti, J.E. Miraglia, Phys. Rev. A **21**, 572 (1980)
17. M. Brauner, J.S. Briggs, H. Klar, J. Phys. B **22**, 2265 (1989)
18. Dz. Belkic, *Principles of Quantum Scattering Theory* (Institute of Physics Publishing, Bristol, 2004)
19. A. Erdelyi, W. Magnus, F. Oberhettinger, F.G. Triconi, *Higher Transcendental Functions*, 1st edn. (McGraw-Hill, New York, 1953)
20. J. Fiol, S. Otranto, R.E. Olson, J. Phys. B **39**, L285 (2006)
21. K.A. Kouzakov, S.A. Zaytsev, Y.V. Popov, M. Takahashi, Phys. Rev. A **86**, 032710 (2012)
22. K.A. Kouzakov, S.A. Zaytsev, Y.V. Popov, M. Takahashi, Phys. Rev. A **87**, 046702 (2013)